J.-L. GUERMOND AND L. QUARTAPELLE[1]

On incremental projection methods

1 Introduction

Achieving high order time-accuracy in the approximation of the incompressible Navier–Stokes equations by means of fractional-step projection methods is a nontrivial task. In fact, a basic feature of this kind of method is the uncoupling of the advection and diffusion from the incompressibility condition, with a consequent introduction of a *time-splitting error* in the computed solution. This splitting introduces an error that depends in general on the size of the time step Δt and is independent of how accurately the subproblem of each partial step is approximated. For instance, the time-splitting error is of $\mathcal{O}(\Delta t)$ for the *non*incremental projection method originally proposed by Chorin [2] and Temam [13].

The occurrence of the splitting error represents a serious obstacle to the construction of time-stepping algorithms with an accuracy of $\mathcal{O}((\Delta t)^2)$ or higher within the class of nonincremental projection methods. As a consequence, it is necessary to resort to a fractional-step time discretization different from the nonincremental one adopted originally. An alternative possibility studied in this paper consists in using the *incremental* version of the projection method, also known as *pressure correction method* in the literature. This method was first proposed by Goda [4] in a finite difference context and has been also analyzed by Van Kan [14] in the special case of a MAC computational molecule combined with a Crank–Nicolson time discretization. The analysis of [14] is however rather formal insofar as it shows that the error is of $c(h)(\Delta t)^2$, the constant $c(h)$ being a mesh dependent factor that behaves like $\mathcal{O}(1/h^2)$.

The finite element counterpart of the incremental method with the time derivative approximated by the implicit Euler scheme has been analyzed and implemented by the authors [8, 9]. In particular, numerical tests reported in [9] show that this algorithm has a time-splitting error of $\mathcal{O}((\Delta t)^2)$. As a consequence, the incremental strategy is an appropriate starting point for deriving second-order accurate projection methods.

A method of this class, based on the three-level Backward Difference Formula applied to the momentum equation, has been proposed by the first author [7]. A judicious choice of coefficients in the projection equation leads to an overall unconditional stability, such that, when mixed finite elements are used, no *ad hoc* stabilization technique is needed. The aim of this paper is to report on the theoretical results of [7] and [9] and

[1]in Proc. International Conference Navier-Stokes Equations: Theory and Numerial Methods, (Varenna (Italy), June 2-6, 1997). R. Salvi (Ed.), Pitman, Research Notes in Mathematics Series Vol. **388**, (1998), 277-288.

to illustrate the second-order accuracy of the proposed method by means of numerical tests.

The paper is organized as follows. First, the Navier–Stokes problem is stated and some notation is introduced. Then, in section 2 we review the incremental fractional-step projection method. A semi-implicit unconditionally stable treatment of the nonlinear term is considered. The incompressible projection step is interpreted as a Poisson problem once a clear and explicit distinction is made between the vector spaces which the intermediate and end-of-step velocity fields belong to. The final algorithm is however formulated in terms of only one velocity field, as explicitly shown in Section 3. The weak equations of the fully discretized problem are given in Section 4. In Section 5, the stability and accuracy of the incremental method are also discussed recalling the main result concerning the time-splitting error of the method. Section 6 introduces a second-order time discretization using the three-level Backward Difference Formula combined with a linear extrapolation for the advection field in the nonlinear terms. In Section 7, some numerical results are given to illustrate the stability properties of equal-order and unequal-order spatial interpolations for velocity and pressure. The test calculations show the $\mathcal{O}((\Delta t)^2)$ behavior of the splitting error for the incremental *Euler* scheme and the $\mathcal{O}((\Delta t)^2)$ accuracy of the new three-level BDF method [7]. The last section is devoted to some concluding remarks.

We are hereafter concerned with the time-dependent incompressible Navier–Stokes equations formulated in terms of the primitive variables: velocity $\boldsymbol{u}$ and pressure p (per unit density). The fluid domain Ω is assumed to be smooth, bounded, and connected in two or three dimensions. The formal mathematical statement of the problem is: Find $\boldsymbol{u}$ and p (up to a constant) so that

$$\begin{cases} \dfrac{\partial \boldsymbol{u}}{\partial t} - \nu \nabla^2 \boldsymbol{u} + (\boldsymbol{u} \cdot \boldsymbol{\nabla}) \boldsymbol{u} + \boldsymbol{\nabla} p = \boldsymbol{f}, \\ \boldsymbol{\nabla} \cdot \boldsymbol{u} = 0, \\ \boldsymbol{u}_{|\partial\Omega} = \boldsymbol{b}, \\ \boldsymbol{u}_{|t=0} = \boldsymbol{u}_0, \end{cases} \tag{1.1}$$

where ν is the viscosity, $\boldsymbol{f}$ is a known body force, $\boldsymbol{b}$ is the velocity prescribed on the boundary $\partial\Omega$, and $\boldsymbol{u}_0$ is the divergence-free initial velocity field. The boundary and the data are assumed to be regular enough and to satisfy all the compatibility conditions needed for a smooth solution to exist for all time. For simplicity, only a Dirichlet boundary condition for velocity is considered here, but more general boundary conditions can be handled by the techniques presented below (see [9]).

2 The incremental fractional-step algorithm

The incremental version of the fractional-step method consists in making explicit the pressure at the viscous step and correcting it at the projection step by evaluating a pressure increment to enforce the incompressibility condition. For the sake of completeness, we briefly restate some results established in [6, 9] and introduce the necessary notations. In particular we focus on the difference in terms of functional setting existing between the two substeps of the method, namely the viscous step and the projection step. This distinction leads to consider two different vector spaces for approximating the intermediate velocity and the end-of-step velocity. It is shown in the next sections that the distinction between the two velocity functional spaces plays a key role in the convergence analysis of the fully discrete method as well as in its practical implementation.

Setting $\boldsymbol{u}^0 = \boldsymbol{u}_0$ and assuming p^0 to be known, for $k \geq 0$ solve the following two problems: First, consider the advection–diffusion step

$$\left\{ \begin{array}{l} \dfrac{\boldsymbol{u}^{k+1} - i^{\,\mathrm{t}}\, \widehat{\boldsymbol{u}}^k}{\Delta t} - \nu \nabla^2 \boldsymbol{u}^{k+1} + (\boldsymbol{u}^k \boldsymbol{\cdot} \boldsymbol{\nabla}) \boldsymbol{u}^{k+1} + \tfrac{1}{2} (\boldsymbol{\nabla} \boldsymbol{\cdot} \boldsymbol{u}^k) \boldsymbol{u}^{k+1} = \boldsymbol{f}^{k+1} - \boldsymbol{\nabla} p^k, \\ \boldsymbol{u}^{k+1}{}_{|\partial\Omega} = \boldsymbol{b}^{k+1}; \end{array} \right. \tag{2.1}$$

then, perform the projection step in the following incremental (pressure-correction) form:

$$\left\{ \begin{array}{l} \dfrac{\widehat{\boldsymbol{u}}^{k+1} - i\, \boldsymbol{u}^{k+1}}{\Delta t} + \widehat{\boldsymbol{\nabla}} (p^{k+1} - p^k) = 0, \\ \widehat{\boldsymbol{\nabla}} \boldsymbol{\cdot} \widehat{\boldsymbol{u}}^{k+1} = 0, \\ \boldsymbol{n} \boldsymbol{\cdot} \widehat{\boldsymbol{u}}^{k+1}{}_{|\partial\Omega} = \boldsymbol{n} \boldsymbol{\cdot} \boldsymbol{b}^{k+1}. \end{array} \right. \tag{2.2}$$

It is important to note the structural difference existing between the viscous step (2.1) and the projection phase of (2.2) of the calculation. The first half-step constitutes an elliptic boundary value problem for an intermediate velocity $\boldsymbol{u}^{k+1}$ accounting for viscosity and convection, whereas the second half-step represents an essentially inviscid problem which determines the end-of-step divergence-free velocity field $\widehat{\boldsymbol{u}}^{k+1}$ together with a suitable approximation of the pressure increment $(p^{k+1} - p^k)$. As a consequence, boundary conditions of a different kind are imposed on the velocity fields that are calculated in the two half-steps. Accordingly, the two operators $\boldsymbol{\nabla}\boldsymbol{\cdot}$ and $\widehat{\boldsymbol{\nabla}}\boldsymbol{\cdot}$ occurring in the two steps are distinct since they act on vector fields belonging to spaces which are endowed with very different regularities, namely, $\boldsymbol{H}^1$ and $\boldsymbol{H}^{\mathrm{div}}$ (or possibly $\boldsymbol{L}^2$), respectively.

The presence of two velocity spaces requires to introduce the injection operator $i : \boldsymbol{H}^1_0 \longrightarrow \boldsymbol{H}^{\mathrm{div}}_0$ and its transpose i^{t}, [5, 6]. Indeed, $\widehat{\boldsymbol{\nabla}}\boldsymbol{\cdot} : \boldsymbol{H}^{\mathrm{div}}_0 \longrightarrow L^2$ is an extension of $\boldsymbol{\nabla}\boldsymbol{\cdot} : \boldsymbol{H}^1_0 \longrightarrow L^2$ in the sense that we have the remarkable property:

$$\widehat{\boldsymbol{\nabla}}\boldsymbol{\cdot}\, i = \boldsymbol{\nabla}\boldsymbol{\cdot} \qquad \text{and} \qquad i^{\,\mathrm{t}} \widehat{\boldsymbol{\nabla}} = \boldsymbol{\nabla}\,.$$

This distinction may seem unduly pedantic in the context of the spatially continuous problem, but it proves to be relevant when it comes to discretizing the equations in space.

By applying $\widehat{\boldsymbol{\nabla}}\boldsymbol{\cdot}$ to the first equation of (2.2), we obtain the following Poisson equation for the pressure variation $(p^{k+1}-p^k)$:

$$\left\{\begin{array}{l} -\widehat{\nabla}^2(p^{k+1}-p^k) = -(\Delta t)^{-1}\,\boldsymbol{\nabla}\boldsymbol{\cdot}\,\boldsymbol{u}^{k+1}, \\ \dfrac{\partial(p^{k+1}-p^k)}{\partial n}_{|\partial\Omega} = 0, \end{array}\right. \tag{2.3}$$

where we have used $\widehat{\boldsymbol{\nabla}}\boldsymbol{\cdot}\, i = \boldsymbol{\nabla}\boldsymbol{\cdot}$. Once p^{k+1} is known, the end-of-step velocity is given by the explicit relation

$$\widehat{\boldsymbol{u}}^{k+1} = i\,\boldsymbol{u}^{k+1} - \Delta t\,\widehat{\boldsymbol{\nabla}}(p^{k+1}-p^k). \tag{2.4}$$

Note that, insofar as the pressure increment solution of the Poisson equation is in H^1, $\widehat{\boldsymbol{\nabla}}(p^{k+1}-p^k)$ belongs to $\boldsymbol{L}^2$; as a result, $\widehat{\boldsymbol{u}}^{k+1}$ should *not* be expected *a priori* to have more regularity than that of $\boldsymbol{H}^{\rm div}$ (which is lower than that of $\boldsymbol{H}^1$).

The time integration scheme chosen in the momentum equation is fully implicit for the viscous term and semi-implicit for the advection term. To guarantee unconditional stability, *i.e.*, to avoid any restriction on the time step Δt, the advection term $(\boldsymbol{v}\boldsymbol{\cdot}\boldsymbol{\nabla})\boldsymbol{u}$ has been replaced by its well known skew-symmetric form $(\boldsymbol{v}\boldsymbol{\cdot}\boldsymbol{\nabla})\boldsymbol{u} + \frac{1}{2}(\boldsymbol{\nabla}\boldsymbol{\cdot}\boldsymbol{v})\boldsymbol{u}$, see *e.g.*, Temam [12] or Quarteroni and Valli [10]. Note that, since the skew-symmetry of the advection term relies on the fact that $\boldsymbol{v}$ is divergence free, one could imagine using $\widehat{\boldsymbol{u}}^k$ as the advection field and writing the advection term in the form $(\widehat{\boldsymbol{u}}^k\boldsymbol{\cdot}\boldsymbol{\nabla})\boldsymbol{u}^{k+1}$ for $\widehat{\boldsymbol{u}}^k$ is divergence free. Actually, this form is not natural since the theoretical analysis shows that $\widehat{\boldsymbol{u}}$ is not regular enough for $(\widehat{\boldsymbol{u}}^k\boldsymbol{\cdot}\boldsymbol{\nabla})\boldsymbol{u}^{k+1}$ to be controlled by means of the usual Sobolev inequalities. This theoretical remark leads quite naturally to formulate a very simple projection method, with the end-of-step velocity eliminated completely from the final algorithm, as shown below.

3 Elimination of the end-of-step velocity

The final velocity $\widehat{\boldsymbol{u}}^{k+1}$ is made to disappear from the fractional-step algorithm by substituting its expression (2.4) into the equation of the (next) viscous step, since we have

$$\begin{aligned} i^{\rm t}\,\widehat{\boldsymbol{u}}^k &= i^{\rm t}[i\,\boldsymbol{u}^k - \Delta t\,\widehat{\boldsymbol{\nabla}}(p^k - p^{k-1})] \\ &= i^{\rm t}\,i\,\boldsymbol{u}^k - \Delta t\,i^{\rm t}[\widehat{\boldsymbol{\nabla}}(p^k - p^{k-1})] \\ &= \boldsymbol{u}^k - \Delta t\,\boldsymbol{\nabla}(p^k - p^{k-1}), \end{aligned}$$

where we have made use of the property $i^{\mathrm{t}}\widehat{\boldsymbol{\nabla}} = \boldsymbol{\nabla}$. This argument is purely formal here but plays a fundamental role in the spatially discrete case. By virtue of this result, the viscous step problem can be rewritten in the simpler, but strictly equivalent, form:

$$\left\{\begin{array}{l} \dfrac{\boldsymbol{u}^{k+1}-\boldsymbol{u}^{k}}{\Delta t} - \nu\nabla^2\boldsymbol{u}^{k+1} + (\boldsymbol{u}^{k}\boldsymbol{\cdot}\boldsymbol{\nabla})\boldsymbol{u}^{k+1} \\ \qquad\qquad + \frac{1}{2}(\boldsymbol{\nabla}\boldsymbol{\cdot}\boldsymbol{u}^{k})\boldsymbol{u}^{k+1} = \boldsymbol{f}^{k+1} - \boldsymbol{\nabla}(2p^{k}-p^{k-1}), \\ \\ \boldsymbol{u}^{k+1}{}_{|\partial\Omega} = \boldsymbol{b}^{k+1}. \end{array}\right. \tag{3.1}$$

4 Fully discretized equations

Let us introduce a finite element approximation $\boldsymbol{X}_{0,h} \subset \boldsymbol{H}^1_0$ for the intermediate velocity $\boldsymbol{u}_h$ and $N_h \subset H^1$ for the pressure p_h, each pressure field being defined up to a constant. Let the polynomial order of interpolation for the velocity be denoted by ℓ (≥ 1) and that for the pressure by ℓ', with $\max(\ell-1,1) \leq \ell' \leq \ell$.

The weak formulation of the advection–diffusion step (3.1) reads: For $k \geq 0$, find $\boldsymbol{u}_h^{k+1} \in \boldsymbol{X}_{\boldsymbol{b}^{k+1},h}$ such that, for all $\boldsymbol{v}_h \in \boldsymbol{X}_{0,h}$,

$$\begin{aligned} \left(\frac{\boldsymbol{u}_h^{k+1}-\boldsymbol{u}_h^{k}}{\Delta t}, \boldsymbol{v}_h\right) + \nu\,(\boldsymbol{\nabla}\boldsymbol{u}_h^{k+1}, \boldsymbol{\nabla}\boldsymbol{v}_h) + ((\boldsymbol{u}_h^{k}\boldsymbol{\cdot}\boldsymbol{\nabla})\boldsymbol{u}_h^{k+1},\, \boldsymbol{v}_h) \\ + \tfrac{1}{2}(\boldsymbol{\nabla}\boldsymbol{\cdot}\boldsymbol{u}_h^{k},\, \boldsymbol{u}_h^{k+1}\boldsymbol{\cdot}\boldsymbol{v}_h) = (\boldsymbol{f}^{k+1}, \boldsymbol{v}_h) - (\boldsymbol{\nabla}(2p_h^{k}-p_h^{k-1}), \boldsymbol{v}_h). \end{aligned} \tag{4.1}$$

The intermediate velocity $\boldsymbol{u}_h^1$ at the first time step is also evaluated from equation (4.1) where by convention we set $p_h^{-1} = p_h^0$.

The projection step has a unique expression only once the functional space for the end-of-step velocity is chosen. It is shown in [5, 6] that many options are possible; one of the simplest consists in selecting $\widehat{\boldsymbol{u}}_h^{k+1}$ in $\boldsymbol{X}_h + \boldsymbol{\nabla}N_h$. Given this particular choice, it can be proven that the operator $\widehat{\boldsymbol{\nabla}}_h$, the discrete counterpart of $\widehat{\boldsymbol{\nabla}}$, coincides exactly with the restriction to N_h of the gradient operator (in terms of distributions); as a result, the projection step takes the following form: For $k \geq 0$, find $(p_h^{k+1}-p_h^k) \in N_h$ such that, for all $q_h \in N_h$,

$$(\boldsymbol{\nabla}(p_h^{k+1}-p_h^{k}), \boldsymbol{\nabla}q_h) = -(\Delta t)^{-1}\,(\boldsymbol{\nabla}\boldsymbol{\cdot}\boldsymbol{u}_h^{k+1}, q_h). \tag{4.2}$$

It must be emphasized that a basic aspect of the method is the introduction of *two different* spaces for representing the velocity computed in each of the two (half-)steps of the method. In fact, the discrete velocity field that is solution of the projection step belongs to a space of vector functions $(\boldsymbol{X}_h + \boldsymbol{\nabla}N_h)$ which are discontinuous at the interfaces of the finite elements. More precisely, the normal component of the end-of-step velocity $\widehat{\boldsymbol{u}}^{k+1}$ is discontinuous at the interfaces between the (pressure) elements. Although this choice may seem peculiar, it is the most natural in the context of

projection schemes based on the Poisson equation for pressure or pressure increment. Note, however, that the discrete end-of-step velocity is never explicitly referenced in the numerical algorithm which is formulated in terms of the intermediate velocity only.

Other choices of the functional space for the end-of-step velocity are possible. For instance, one may pick $\widehat{\boldsymbol{u}}_h^{k+1}$ in $\boldsymbol{X}_{\boldsymbol{b}^{k+1},h}$. This choice is permitted, provided that the inf-sup condition between $\boldsymbol{X}_h$ and N_h is satisfied; however, it is not optimal and yields a discrete problem for the pressure involving the inverse of the mass matrix. The reader is referred to [6] for a review of other possible choices.

5 Stability and convergence

We want to discuss now the stability and convergence properties of the incremental projection scheme (4.1) and (4.2). Since the incompressibility constraint is enforced through an *uncoupled* pressure Poisson problem, one may think that in principle any spatial discretization for approximating elliptic problems is admissible. More precisely, since the two steps (4.1) and (4.2) are fully uncoupled, it is conceivable to solve these problems by any H^1-conformal finite element technique without the two approximation spaces $\boldsymbol{X}_{0,h}$ and N_h being subordinate to the inf-sup condition. However, this view (widely shared in the literature) is false since the stability provided by the Poisson equation of the incremental scheme only applies to the pressure variation. This is a critical difference with the nonincremental projection method which guarantee some sort of stability on the instantaneous pressure field itself, but only for Δt large enough. As a matter of facts, the nonincremental technique trades accuracy for (conditional) stability. This feature is clearly illustrated by the numerical tests to be presented in section 7.

The description of the incremental fractional-step projection method is concluded by recalling the following result established in [8].

Theorem 1 *Under convenient regularity assumptions on the data $\boldsymbol{f}$, $\boldsymbol{u}_0$, $\boldsymbol{b}$, and provided the inf-sup condition is satisfied, the solution to the incremental projection scheme (4.1)-(4.2) satisfies the error bounds:*

$$\max_{0\le k\le K}\left\|\boldsymbol{u}_h^k-\boldsymbol{u}(t^k)\right\|_0+\max_{0\le k\le K}\left\|\widehat{\boldsymbol{u}}_h^k-\boldsymbol{u}(t^k)\right\|_0\le c[\boldsymbol{u},p](\Delta t+h^{\ell+1}),\tag{5.1}$$

$$\max_{0\le k\le K}\left\|\boldsymbol{u}_h^k-\boldsymbol{u}(t^k)\right\|_1+\max_{0\le k\le K}\left\|p_h^k-p(t^k)\right\|_0\le c[\boldsymbol{u},p](\Delta t+h^{\ell}),\tag{5.2}$$

as $\Delta t\to 0$ and $h\to 0$, where ℓ is the interpolation degree of the velocity.

These error estimates show that the incremental algorithm achieves an $\mathcal{O}(\sqrt{\Delta t})$ increase of accuracy with respect to the nonincremental algorithm. Moreover, let us denote by $(\boldsymbol{w}_h,q_h)$ the solution of the fully coupled problem: set $\boldsymbol{w}_h^0=\boldsymbol{u}_h^0$, and for

$k \geq 0$ define $\boldsymbol{w}_h^{k+1} \in \boldsymbol{X}_{\boldsymbol{b}^{k+1},h}$ and $q_h^{k+1} \in N_h$ such that,

$$\left\{ \begin{array}{l} \left(\dfrac{\boldsymbol{w}_h^{k+1}-\boldsymbol{w}_h^k}{\Delta t}, \boldsymbol{v}_h\right) + \nu\,(\boldsymbol{\nabla}\boldsymbol{w}_h^{k+1}, \boldsymbol{\nabla}\boldsymbol{v}_h) + ((\boldsymbol{w}_h^k \cdot \boldsymbol{\nabla})\boldsymbol{w}_h^{k+1},\, \boldsymbol{v}_h) \\ \qquad + \frac{1}{2}(\boldsymbol{\nabla}\cdot \boldsymbol{w}_h^k,\, \boldsymbol{w}_h^{k+1}\cdot \boldsymbol{v}_h) - (q_h^{k+1}, \boldsymbol{\nabla}\cdot \boldsymbol{v}_h) = (\boldsymbol{f}^{k+1}, \boldsymbol{v}_h), \quad \forall \boldsymbol{v}_h \in \boldsymbol{X}_{0,h}, \\ (\boldsymbol{\nabla}\cdot \boldsymbol{w}_h^{k+1}, r_h) = 0, \qquad\qquad \forall r_h \in N_h. \end{array} \right. \tag{5.3}$$

The solution of this problem can be obtained by various means; for instance, it can be calculated by solving iteratively the Uzawa operator (see *e.g.* Temam [12] for an introduction to this technique). The computational cost for evaluating the coupled solution, $(\boldsymbol{w}_h, q_h)$, is in general much higher than that needed for evaluating the uncoupled solution $(\boldsymbol{u}_h, p_h)$ of (4.1)-(4.2). Indeed, it is this difference in the computational costs that is at the origin of the popularity of fractional-step projection methods. The difference between $\boldsymbol{w}_h$ and $\boldsymbol{u}_h$ is the error induced by the uncoupling of the incompressibility constraint; this difference is conventionally called the *time-splitting error*. It is proved in Guermond [7] that the time-splitting error induced by the incremental algorithm is indeed $\mathcal{O}((\Delta t)^2)$:

Theorem 2 *Provided the inf-sup condition is satisfied, the solution $(\boldsymbol{u}_h, p_h)$ to the incremental projection scheme (4.1)-(4.2) satisfies the following bounds:*

$$\|\boldsymbol{u}_h - \boldsymbol{w}_h\|_{l^2(\boldsymbol{L}^2)} + \|\widehat{\boldsymbol{u}}_h - \boldsymbol{w}_h\|_{l^2(\boldsymbol{L}^2)} \leq c[\boldsymbol{w}_h, q_h](\Delta t)^2 \tag{5.4}$$

as $\Delta t \to 0$, where $(\boldsymbol{w}_h, q_h)$ is the solution to the coupled problem (5.3).

This result implies that second order accuracy in time is possible if the first-order time stepping is replaced by a second-order scheme, for instance the trapezoidal rule or the three-level backward difference (BDF) formula to be discussed in the next section.

6 A second-order BDF projection scheme

The three-level BDF is chosen to benefit from better stability properties than those of the commonly used Crank–Nicolson scheme, which is known to be marginally stable. The unconditional stability is maintained in the nonlinear regime by using the skew-symmetric form of the advection term evaluated semi-implicitly by means of a linear extrapolation in time of the new advection velocity. The scheme reads:

$$\left\{ \begin{array}{l} \dfrac{3\boldsymbol{u}^{k+1} - 4i^{\mathrm{t}}\widehat{\boldsymbol{u}}^k + i^{\mathrm{t}}\widehat{\boldsymbol{u}}^{k-1}}{2\Delta t} - \nu\nabla^2\boldsymbol{u}^{k+1} + (\boldsymbol{u}_\star^{k+1}\cdot\boldsymbol{\nabla})\boldsymbol{u}^{k+1} \\ \qquad\qquad + \frac{1}{2}(\boldsymbol{\nabla}\cdot\boldsymbol{u}_\star^{k+1})\boldsymbol{u}^{k+1} = \boldsymbol{f}^{k+1} - \boldsymbol{\nabla}p^k, \\ \boldsymbol{u}^{k+1}{}_{|\partial\Omega} = \boldsymbol{b}^{k+1}, \end{array} \right. \tag{6.1}$$

having introduced the linearly extrapolated velocity

$$\boldsymbol{u}_\star^{k+1} = 2\boldsymbol{u}^k - \boldsymbol{u}^{k-1}; \tag{6.2}$$

then, perform the projection step in the following incremental form:

$$\begin{cases} \dfrac{3\widehat{\boldsymbol{u}}^{k+1} - 3i\,\boldsymbol{u}^{k+1}}{2\Delta t} + \widehat{\boldsymbol{\nabla}}(p^{k+1} - p^k) = 0, \\ \widehat{\boldsymbol{\nabla}}\cdot\,\widehat{\boldsymbol{u}}^{k+1} = 0, \\ \boldsymbol{n}\cdot\widehat{\boldsymbol{u}}^{k+1}{}_{|\partial\Omega} = \boldsymbol{n}\cdot\boldsymbol{b}^{k+1}. \end{cases} \tag{6.3}$$

Once the intermediate velocities $\widehat{\boldsymbol{u}}^k$ and $\widehat{\boldsymbol{u}}^{k-1}$ are eliminated, the first step takes the following form in practice:

$$\begin{cases} \dfrac{3\boldsymbol{u}^{k+1} - 4\boldsymbol{u}^k + \boldsymbol{u}^{k-1}}{2\Delta t} - \nu\nabla^2\boldsymbol{u}^{k+1} + (\boldsymbol{u}_\star^{k+1}\cdot\boldsymbol{\nabla})\boldsymbol{u}^{k+1} \\ \qquad\qquad + \frac{1}{2}(\boldsymbol{\nabla}\cdot\,\boldsymbol{u}_\star^{k+1})\boldsymbol{u}^{k+1} = \boldsymbol{f}^{k+1} - \frac{1}{3}\boldsymbol{\nabla}(7p^k - 5p^{k-1} + p^{k-2}), \\ \boldsymbol{u}^{k+1}{}_{|\partial\Omega} = \boldsymbol{b}^{k+1}. \end{cases} \tag{6.4}$$

$$\begin{cases} -\widehat{\nabla}^2(p^{k+1} - p^k) = -\dfrac{3}{2\Delta t}\,\boldsymbol{\nabla}\cdot\,\boldsymbol{u}^{k+1}, \\ \dfrac{\partial(p^{k+1} - p^k)}{\partial n}{}_{|\partial\Omega} = 0, \end{cases} \tag{6.5}$$

The following convergence result is proven in Guermond [7]:

Theorem 3 *Under convenient regularity assumptions on the data $\boldsymbol{f}$, $\boldsymbol{u}_0$, $\boldsymbol{b}$, and provided the inf-sup condition is satisfied, the solution to the three-level BDF projection scheme (6.4)-(6.5) satisfies the error bounds:*

$$\|\boldsymbol{u}_h - \boldsymbol{u}\|_{l^2(\boldsymbol{L}^2)} + \|\widehat{\boldsymbol{u}}_h - \boldsymbol{u}\|_{l^2(\boldsymbol{L}^2)} \leq c[\boldsymbol{u}, p][(\Delta t)^2 + h^{\ell+1}] \tag{6.6}$$

as $\Delta t \to 0$ and $h \to 0$.

7 Numerical results

For the numerical illustrations, we rely upon the well known standard driven cavity problem [1]. We have taken a Reynolds number equal to 100, which is well documented in the literature. All the linear systems involved in the algorithm are solved by direct methods for large sparse systems of linear equations. The calculations are performed on uniform meshes.

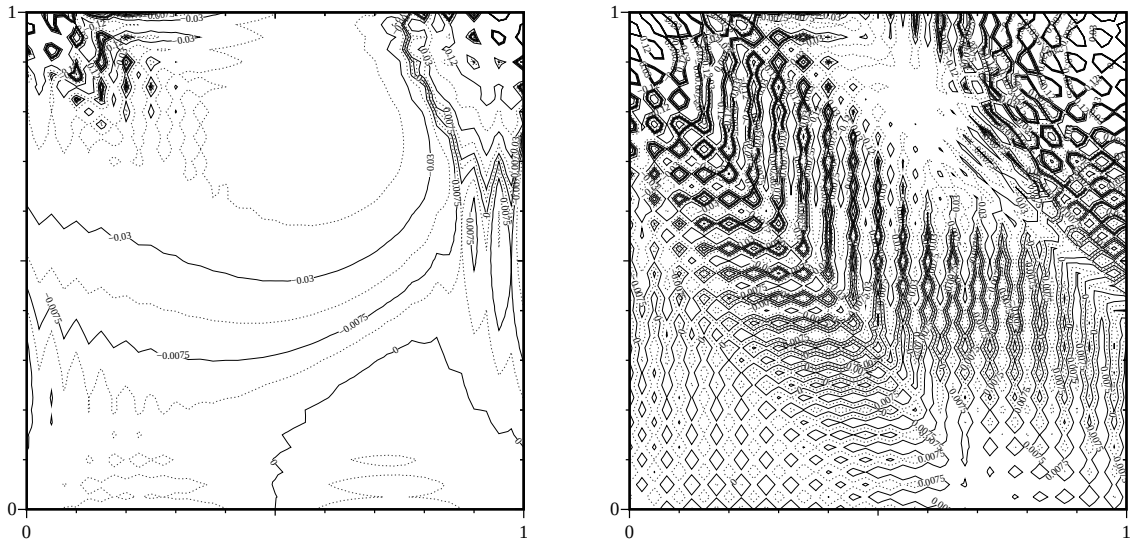

Figure 1: Pressure field in the driven cavity $R = 100$: Incremental method with equal-order P_1/P_1 interpolation. Left $\Delta t = 0.1$ and right $\Delta t = 0.01$.

To illustrate the fact that the inf-sup condition is a necessary condition for the incremental projection technique to work properly, we show some counter-examples. We consider first the incremental method with an equal-order P_1/P_1 interpolation using a mesh of 2×40^2 equal triangles. Recall that the P_1/P_1 element does not satisfy the inf-sup condition. The steady-state pressure fields computed with two representative time steps $\Delta t = 0.1$ and $\Delta t = 0.01$ are shown in Figure 1. Severe node-to-node oscillations clearly appear in both cases, the worst case corresponding to the smaller time-step. These results confirm that the inf-sup compatibility condition must be satisfied for the incremental method to work properly, although the use of large time steps can make this necessity less evident.

We emphasize that a refinement of the mesh for the equal-order interpolation is not capable of curing the spatial oscillations, as clearly demonstrated by Figure 2 for $\Delta t = 0.01$. Here we compare the solution obtained by the equal-order P_1/P_1 approximation on a mesh of 2×80^2 of equal triangles with that obtained by the mixed P_1/P_2 approximation on a mesh of 2×40^2 linear/parabolic elements for pressure/velocity.

To illustrate the capability of the incremental method to provide $\mathcal{O}((\Delta t)^2)$ time splitting error as predicted in Theorem 2, we conduct a convergence test on a fixed mesh by comparing the solution calculated by the projection method to that of the coupled system (5.3) obtained by solving the Uzawa operator. The tests are performed on the driven cavity using a unstructured P_1/P_2 triangulation consisting of ≈ 400 P_2-nodes. In Figure 7, we plot the errors on velocity and pressure measured, respectively, by the maximum in time of the energy norm, *i.e.*, $l^\infty(0,1;\boldsymbol{L}^2)$, for the velocity (solid line) and by the energy norm in space and time, *i.e.*, $l^2(0,1;L^2)$, for the pressure

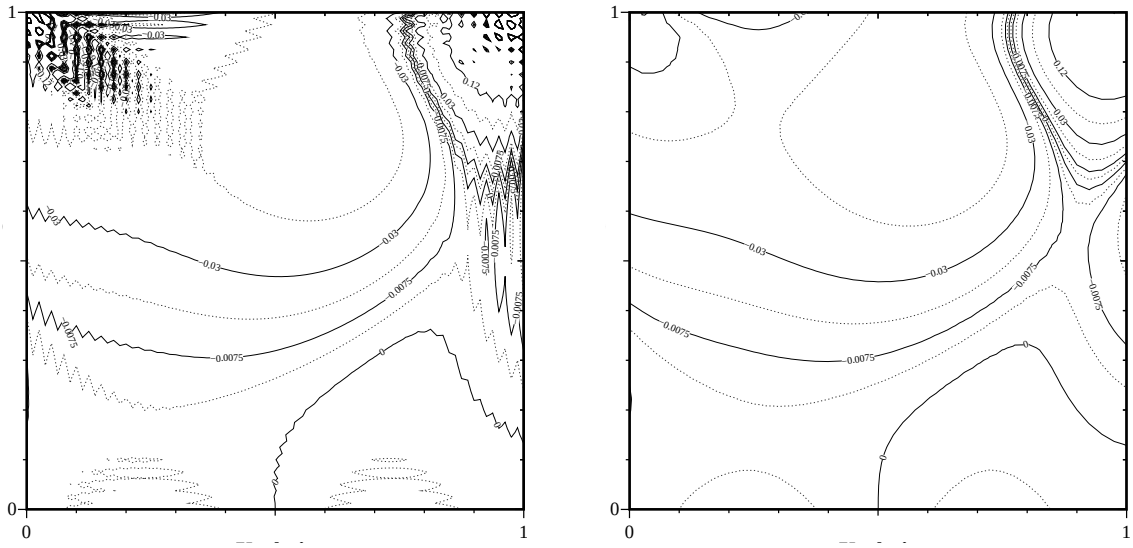

Figure 2: Pressure field in the driven cavity $R = 100$ on finer meshes: Incremental method with equal-order P_1/P_1 interpolation on a 2×80^2 mesh (left) and mixed P_1/P_2 interpolation on a 2×40^2 mesh (right); $\Delta t = 0.01$.

(dotted line). The dashed line corresponds to second-order convergence in time. The present test clearly shows that the incremental scheme yields a time splitting error of $\mathcal{O}((\Delta t)^2)$.

To verify the theoretical $\mathcal{O}((\Delta t)^2)$ accuracy of the three-level BDF scheme predicted by Theorem 3, this scheme has been tested with the following analytical solution in the unit square $\Omega = [0,1]^2$:

$$\begin{cases} u_x = -\cos x \sin y \, g(t), \\ u_y = \sin x \cos y \, g(t), \\ p = -\frac{1}{4}[\cos(2x) + \cos(2y)] \, g^2(t), \end{cases}$$

where $g(t) = \sin(2t)$. Setting the velocity in the formal form $\boldsymbol{u} = \overline{\boldsymbol{u}}(x,y)g(t)$, then the source term corresponding to the Navier–Stokes equations is $\boldsymbol{f} = \overline{\boldsymbol{u}}(x,y)[g'(t) + 2g(t)/R]$. The Reynolds number is set to 100 and we use a mesh of 2×40^2 P_1/P_2 triangles. Figure 4 shows the maximum value in time, over $0 \le t \le 1.5$, of the error in the L^2 norm for the pressure and the error in the H^1 and L^2 norms for the velocity; the tests have been carried out on two P_1/P_2 meshes composed of 2×20^2 P_2-triangles and 2×40^2 P_2-triangles respectively. The different saturations of the errors as $\Delta t \to 0$ are due to the spatial discretization error, which is of order h^2 for the velocity (resp. pressure) in the H^1 (resp. L^2) norm, while it is of order h^3 for the velocity in the L^2

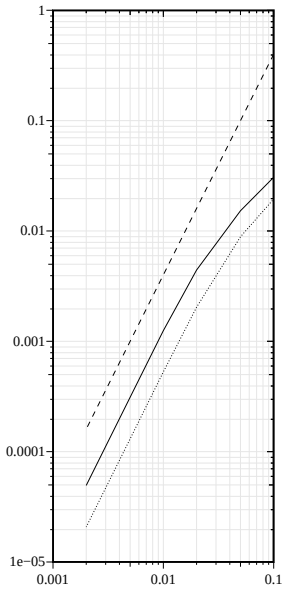

Figure 3: Splitting error vs. Δt: velocity (solid line) and pressure (dotted line); Second-order slope (dashed line). Driven cavity problem at $R = 100$, with P_1/P_2 interpolation with ≈ 400 P_2-nodes.

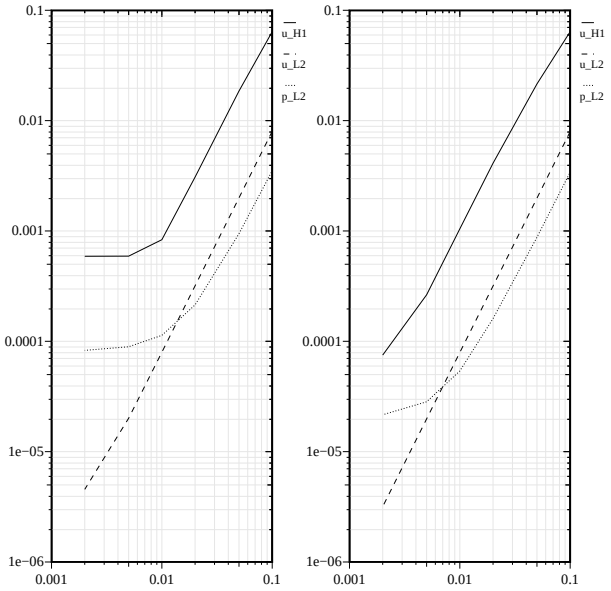

Figure 4: Convergence tests for the second-order BDF projection method, with mixed P_1/P_2 interpolation. Analytical test problem for $R = 100$; finite element mesh of 2×20^2 P_2-triangles (left) and 2×40^2 P_2-triangles (right).

norm. This convergence test confirms that the incremental projection method retains the optimal space approximation property of the finite elements and introduces only a second-order error in time as expected.

8 Conclusions

The convergence as h and $\Delta t \to 0$, where h is the mesh size and Δt is the time step, is the basic issue in any numerical method for the computation of transient flows. For the approximation of the incompressible Navier–Stokes equations by means of projection methods, the convergence analysis is complicated by the occurrence of a time-splitting error brought about by the fractional character of the time discretization. It is shown in this paper that the time splitting error induced by uncoupling the viscosity from incompressibility is of $\mathcal{O}((\Delta t)^2)$ if the pressure is dealt with in an incremental form.

The three-level backward difference formula has been adopted and combined with the incremental version of the projection method to obtain an overall second-order accurate true projection method. An $\mathcal{O}((\Delta t)^2)$ convergence theorem is given and this result is illustrated by numerical tests. The functional setting that comes into play involves two different vector spaces endowed with quite different regularities for the

velocity fields implied in the two half-steps of the method.

Though, by naively looking at each substep of the incremental projection method, one may conceive solving each subproblem by any H^1-conformal finite element technique without the two approximation spaces satisfying the inf-sup condition, we have shown by giving counter-examples that this idea is wrong. Unwanted spurious modes for pressure (and possibly also for velocity) are *a priori* avoided by resorting to mixed finite element approximations, for example, the classical P_1/P_2 polynomial approximation. Respecting the inf-sup condition yields an unconditionally stable projection method of second-order time accuracy which needs no help from artificial stabilization techniques.

References

[1] Burggraf, O R, *J. Fluid Mech.*, **24**, (1966), 113–151.

[2] Chorin, A J, *Math. Comp.*, **22**, (1968), 745–762.

[3] Chorin, A J, *Math. Comp.*, **23**, (1969), 341–353.

[4] Goda, K, *J. Comput. Phys.*, **30**, (1979), 76–95.

[5] Guermond, J-L, *C. R. Acad. Sc. Paris*, Série I, **319**, (1994), 887–892.

[6] Guermond, J-L, *Modél. Math. Anal. Numér.* (M^2AN), **30**, (1996), 637–667.

[7] Guermond, J-L, to appear in *Modél. Math. Anal. Numér.* (M^2AN), (1997).

[8] Guermond, J-L and Quartapelle, L, to appear in *Numer. Math.*, (1997).

[9] Guermond, J-L and Quartapelle, L, *J. Comput. Phys.*, **132**, (1997), 12–33.

[10] Quarteroni, A and Valli, A, *Numerical Approximation of Partial Differential Equations*, Springer Series in Computational Mathematics, **23** Springer-Verlag, 1994.

[11] Rannacher, R, *Lectures Notes in Mathematics*, **1530**, Springer, Berlin, (1992), 167–183.

[12] Temam, R, *Navier–Stokes Equations*, Studies in Mathematics and its Applications, **2**, North-Holland, 1977.

[13] Temam, R, *Bull. Soc. Math. France*, **98**, (1968), 115–152.

[14] Van Kan J, *SIAM J. Sci. Stat. Comput.*, **7**, 1986, 870–891.